CHEMISTRY
A EUROPEAN JOURNAL

DOI: 10.1002/chem.200800186

Functional Macromolecules from Single-Walled Carbon Nanotubes: Synthesis and Photophysical Properties of Short Single-Walled Carbon Nanotubes Functionalised with 9,10-Diphenylanthracene

Carmela Aprile,[a] Roberto Martín,[a] Mercedes Alvaro,[a] Juan C. Scaiano,*[b] and Hermenegildo Garcia*[a]

Abstract: 9,10-Diphenylanthracene (DPA), a well-studied organic chromophore ($\Phi_{fl}=0.98$) that exhibits electroluminescence, has been covalently bound through 2-(ethylthio)ethylamido linkers to the carboxylic acid groups of short, soluble single-walled carbon nanotubes (sSWNTs) of 1 μm average length, and the resulting DPA-functionalised sSWNT (DPA- sSWNT) macromolecular adducts (4.6 wt% DPA content) characterised by solution ^{1}H NMR, Raman and IR spectroscopy and thermogravimetric analysis. Comparison of the quenching of DPA fluorescence (steady-state and time-resolved) and of the transient optical spectra of sSWNTs and DPA-sSWNTs show that the covalent linkage boosts the interaction between the DPA and the sSWNT units. DPA-sSWNTs exhibit emission in the near-IR region from 1100–1400 nm with an enhanced quantum yield ($\Phi=5.7\times10^{-3}$) compared with sSWNTs ($\Phi=3.9\times10^{-3}$).

Keywords: fluorescence · IR spectroscopy · macromolecules · nanotubes · NMR spectroscopy

Introduction

In the last few decades considerable research activity has been focused on developing the chemistry of new carbon allotropes.[1–5] Although the chemistry of fullerenes has become a mature field and a large number of fullerene derivatives have been synthesised,[3–7] there remains much interest in exploiting the potential of carbon nanotubes.[6,8–11] Owing to their nanometric diameter, long aspect ratio, electronic conductivity and mechanical resistance, single-walled carbon nanotubes (SWNTs) are important materials in nanotechnology.[9,10] One of the most important differences between fullerenes and SWNTs is that the former allotropes are discrete, molecular entities that consist of a limited number of carbon atoms, whereas as-produced SWNTs are better considered as the result of the rolling up of a graphene layer with each individual nanotube formed of a countless number of carbon atoms. Thus, SWNTs are "materials" rather than molecular compounds, which makes the preparation of persistent suspensions of SWNTs in common solvents problematic. Soluble, persistent, colloidal suspensions of SWNTs can be prepared by careful chemical cutting of the raw materials to the point that the intractable solid is oxidatively degraded into short pieces of the original nanotube (sSWNT).[12–16]

In comparison to as-synthesised SWNTs, soluble sSWNTs can be readily functionalised by conventional liquid-phase reactions.[11,14,15,17–20] Furthermore, the resulting derivatives can be characterised conveniently by transmission spectroscopy and their structures more firmly established by liquid-phase NMR spectroscopy.[20–23]

Covalent functionalisation of sSWNTs can serve to induce a response in the properties of the nanotube upon stimulus of the attached moiety.[11,18,19,24,25] The ability of nanotubes to respond upon photochemical excitation is one of their most useful properties and may lead to their development for a large variety of applications, for example, as sensors, relays, and photovoltaic and electroluminescent devices.[8,9,26–38] The functionalisation of sSWNTs has emerged as a line of research parallel to that developed in the 1990s

[a] Dr. C. Aprile, R. Martín, Dr. M. Alvaro, Prof. Dr. H. Garcia
Instituto de Tecnología Química CSIC-UPV
Universidad Politécnica de Valencia
Av. de los Naranjos s/n, 46022 Valencia (Spain)
Fax: (+34) 963-877-809
E-mail: hgarcia@quim.upv.es

[b] Prof. Dr. J. C. Scaiano
Department of Chemistry, University of Ottawa
10 Marie Curie, Ottawa K1N 6N5 (Canada)

with the functionalisation of the fullerene allotropic form of carbon.

Herein, we describe the preparation of sSWNTs bearing covalently attached 9,10-diphenylanthracene units (DPA-sSWNTs). In addition to being a basic aromatic hydrocarbon whose photochemistry is well understood, 9,10-diphenylanthracene (DPA) has many interesting properties, such as a very high quantum yield ($\Phi \approx 0.98$) of blue fluorescence ($\lambda_{em} = 410$ nm), and has been used as the reporting unit in chemosensors and in the construction of electroluminescent devices.[39–45] It is believed that the conductive properties of SWNTs can play a positive role in electroluminescence and other phenomena in nanotechnology.[46] In addition to convincing spectroscopic evidence of their synthesis, we have observed the distinctive photochemical behaviour of the resulting DPA-sSWNTs compared with mixtures of the non-bonded, constituent components.

Results and Discussion

Synthesis and characterisation of DPA-sSWNTs: Commercially available high-pressure CO (HiPCO) SWNTs were submitted to a controlled oxidative treatment with a 3:1 mixture of concentrated sulfuric/nitric acids to effect a purification from metallic impurities and to achieve a chemical cut of the long tubes to yield short tubes. In accord with a reported protocol,[12] the resulting sSWNTs have an average length of 1 μm, as determined by TEM (Figure 1). In addition, to effect the cut of the as-synthesised nanotubes into shorter units, it is known that the oxidative chemical treatment also produces some defects on the graphene wall.[47] sSWNTs form indefinitely persistent solutions in water and most common organic solvents, including chlorinated alkanes, DMSO and DMF. Even though colloidal dispersions of sSWNTs do not show a tendency to sedimentation, they can be recovered by filtration through 0.2 μm Nylon filters. Thus, their purification and recovery from soluble impurities is straight forward. Filtered sSWNTs can be easily redispersed, and freeze-dried sSWNTs proved particularly convenient for obtaining an instantaneous soluble sample (>2 mg mL^{-1}).

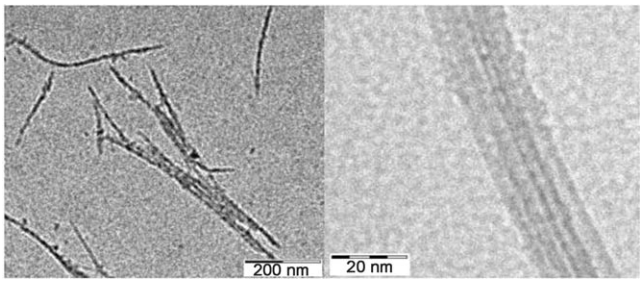

Figure 1. TEM images of sSWNTs at two different magnifications. Left: Aspect ratio of soluble sSWNTs showing an average length of 1 μm. Right: Image showing that the single-walled structure is preserved in sSWNTs and that they are formed by bundles with a width of about 20 nm.

sSWNTs were functionalised by DPA units by using a strategy based on radical-chain addition to styryl units that effects a covalent linkage to the carboxylic groups located at the nanotube tips and the wall defects.[47] Scheme 1 shows the procedure followed for the preparation of DPA-sSWNTs.

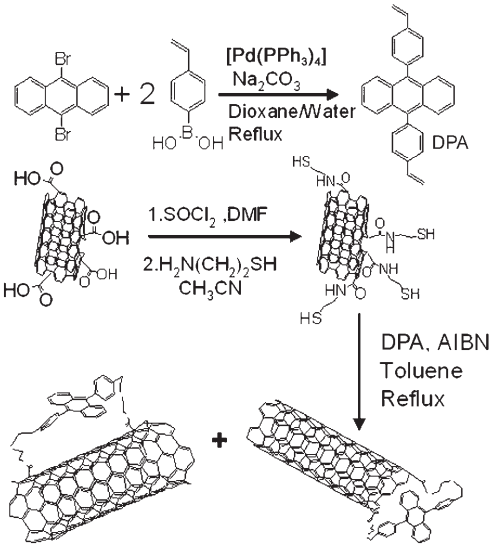

Scheme 1. Synthetic route to DPA-sSWNTs.

The synthetic route requires the preparation of a DPA derivative bearing two styryl units at the 9- and 10-positions. Treatment of the DPA derivative with azobisisobutyronitrile (AIBN) as radical initiator in the presence of mercaptoethyl-functionalised sSWNTs gives rise to DPA-sSWNTs. Our synthetic route relies on the radical addition of thiols to styryl C=C double bonds, a reaction that occurs quantitatively in the absence of oxygen under neutral conditions and moderate temperatures. The radical addition of thiols to C=C double bonds is a strategy that has been widely and successfully used to attach covalently organic units to insoluble inorganic solids such as mesoporous silica.[48] DPA bearing styryl units has been previously reported in the literature and is obtained in high yields by palladium-catalysed Suzuki–Miyaura coupling of 9,10-dibromoanthracene and 4-styrylboronic acid.[49] Mercaptoethylamido-functionalised sSWNTs are in turn obtained by the formation of a peptide bond between the carboxylic groups present in the sSWNTs and mercaptoethanamine. As it is known that in SWNTs carboxylic acids are localised at the tips and defects of the nanotubes,[18,19] our functionalisation approach leaves unaltered the integrity of the graphene walls with respect to those of sSWNTs.

The DPA-sSWNTs were purified by consecutive cycles of filtration through a 0.2 μm Nylon filter, washings and redispersion. A control in which sSWNTs were treated analogously with DPA lacking the terminal C=C double bonds

showed that this purification procedure is sufficient to remove DPA to a level such that this aromatic hydrocarbon cannot be detected by optical or fluorescence spectroscopy.

The DPA-sSWNTs were characterised by transmission spectroscopy. The results are compatible with the covalent attachment of DPA to sSWNTs. The most convincing piece of evidence is the ^{1}H NMR spectrum of a [D_6]DMSO solution of DPA-sSWNTs. Figure 2 shows a comparison of the ^{1}H NMR spectra of DPA and DPA-sSWNTs. As can be seen, although the spectrum of DPA-sSWNTs exhibits the signals expected for the aromatic moiety, the δ values of thee signals are substantially different for DPA and DPA-sSWNTs. We believe that this shift in the aromatic protons is caused by the magnetic anisotropy produced by the sSWNT walls near the DPA units. Given the lack of planarity of DPA, the formation of a non-covalent π–π complex between DPA and sSWNT that could also be responsible for the analogous peak shift seems unlikely in this case. The quality of the ^{1}H NMR spectrum shown in Figure 2 with narrow peaks contrasts with the paucity of NMR spectroscopic data for most functionalised SWNTs and reflects the advantages of soluble compounds.

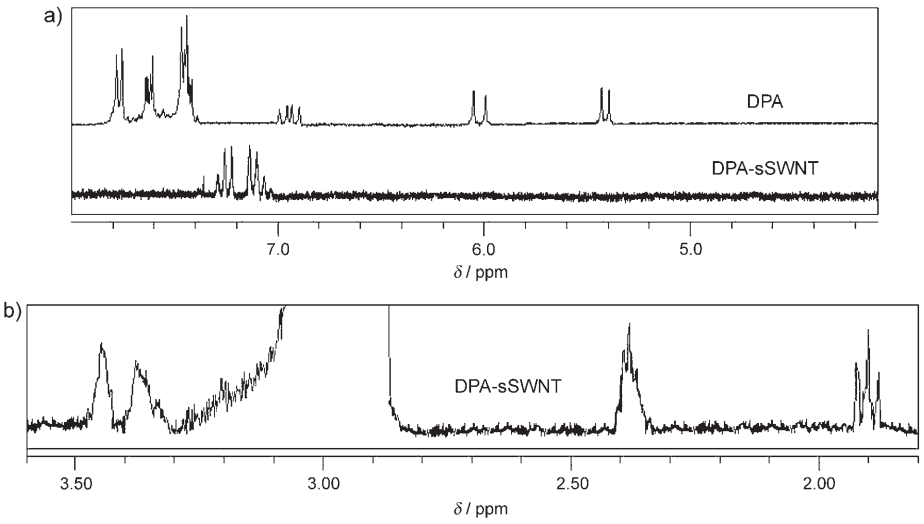

Figure 2. a) ^{1}H NMR spectra of DPA (top) and DPA-sSWNTs in [D_6]DMSO (bottom, 2.5 mg mL^{-1}), showing the similarities of the peaks in the aromatic region. b) Signals in the aliphatic region of the ^{1}H NMR spectrum of DPA-sSWNTs.

The DPA content in DPA-sSWNTs was estimated by combustion chemical analysis. As sSWNTs only contain carbon and oxygen atoms, the percentage of sulfur and nitrogen heteroatoms in the combustion of DPA-sSWNTs allows the loading of DPA units to be estimated at 4.6 wt%. This percentage of photoactive units is not uncommon in carbon nanotubes functionalised through carboxylic acid moieties.[18,19]

Thermogravimetric analyses (TGA) in air show different profiles for pristine SWNTs, sSWNTs and DPA-sSWNTs (Figure 3). Thus, the parent SWNT does not exhibit any

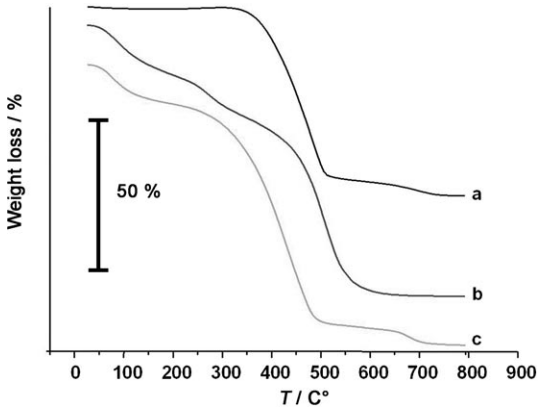

Figure 3. Thermogravimetric profiles obtained in air for a) commercial SWNTs, b) purified sSWNTs and c) DPA-sSWNTs.

weight loss below 305 °C and combustion takes places in the range 305–600 °C with a weight loss of 57 wt%. The rest of the material (43 wt%) present in the commercial SWNT material should be inorganic impurities. In contrast, purification and shortening of the commercial sample gives rise to sSWNTs whose TGA profile gives a total weight loss of 91 wt%. In addition, exothermic weight loss starts at very low temperatures, there being a significant 29.97% weight loss between ambient temperature and 340 °C. This profile is indicative of the absence of inorganic impurities and the presence of a considerable number of defects. In particular, carboxylic acid groups decompose at temperatures below 340 °C. Functionalisation of sSWNTs to form DPA-sSWNTs changes the TGA profile; it is better resolved and shows two clear stages in the weight loss. In particular, the DPA-sSWNTs, with respect to sSWNTs, lose less weight in the region below 200 °C (17.17 vs 12.33 wt% for sSWNTs and DPA-sSWNTs, respectively) and the DPA unit decomposes, together with the combustion of the graphene wall, in the region of 200 to 500 °C (72.09 wt%).

Chemical treatment to obtain sSWNTs and their subsequent functionalisation to DPA-sSWNTs is also reflected in variations in the IR spectra. Figure 4 shows a comparison of the IR spectra of commercial SWNTs, purified sSWNTs and DPA-sSWNTs. As can be seen, chemical cutting introduces a considerable population of OH and CO groups that can be associated with the creation of carboxylic acid groups. Upon functionalisation, the IR spectrum of the DPA-sSWNTs reveals a decrease in the population of the OH

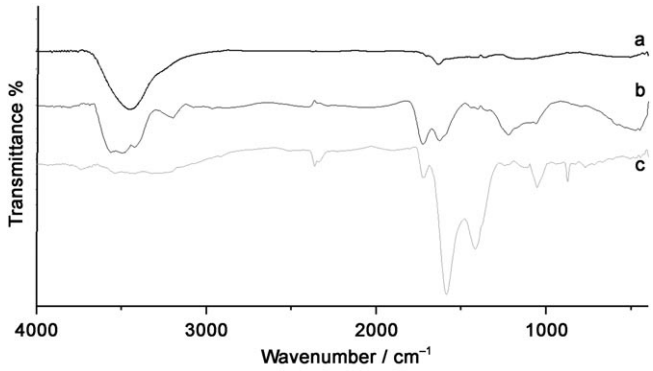

Figure 4. IR spectra of a) commercial SWNTs, b) sSWNTs and c) DPA-sSWNTs.

groups, whereas the CO stretching peak that corresponds to the ester groups is maintained and intense bands in the aromatic region appear.

Raman spectroscopy is a very useful technique for following changes in the graphene structure of SWNTs. Figure 5 shows the Raman spectra of commercial SWNTs, sSWNTs

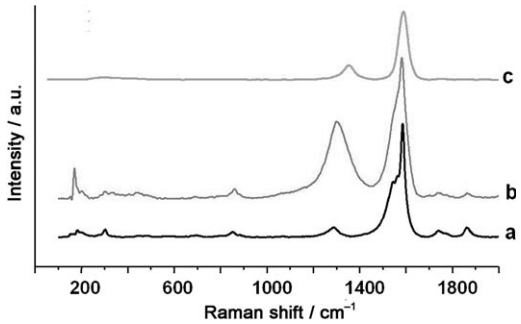

Figure 5. Raman spectra of a) commercial SWNTs, b) sSWNTs and c) DPA-sSWNTs.

and DPA-sSWNTs. The chemical treatment used to purify and cut SWNTs produces a relative increase in the band at 1380 cm^{-1} with respect to the tangential vibration mode at 1605 cm^{-1}. This increase in intensity of the band at 1380 cm^{-1} has been frequently observed when effecting SWNT functionalisation and has been attributed to the creation of defects on the graphene walls.[21,50] Importantly, the peak at 180 cm^{-1}, which corresponds to the radial breathing mode characteristic of single-walled carbon nanotubes, is still observed in the sSWNT sample, which indicates that the morphology of the nanotube has survived the chemical treatment, a fact that we have already highlighted based on the observed TEM images. Finally, note that no peaks corresponding to the diphenylanthracene unit are observed in the Raman spectrum of DPA-sSWNTs. This fact is not surprising considering the low content of DPA in the sample (4.6 wt%) and the dominant sSWNT signal in the Raman spectrum.

Photochemical properties of DPA-sSWNTs: Transmission UV/Vis spectroscopy of aqueous DPA-sSWNT solutions shows the features expected for the additive combination of DPA and sSWNTs in their relative proportions. Thus, sSWNTs exhibit a continuum absorption throughout the wavelength range that corresponds to black carbon. Interestingly, although most samples of SWNTs exhibit absorption peaks in the NIR region that correspond to the van Hove singularities, sSWNTs do not exhibit these bands. There are literature precedents in which non-covalent[51,52] as well as covalent[53] modifications of SWNTs lead to the disappearance of the characteristic van Hove bands. It is also possible that the short lengths and the defects on the walls of the nanotubes in the sSWNTs and DPA-sSWNT are responsible for the disappearance of the van Hove bands. On the other hand, DPA has a structured absorption band with maxima at 356, 375 and 397 nm. In agreement with its constituents, the optical spectrum of DPA-sSWNTs shows a continuum absorption with small peaks at the wavelengths expected for DPA (Figure 6).

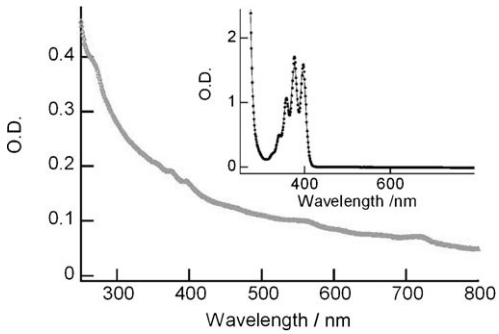

Figure 6. UV/Vis spectrum of a solution of DPA-sSWNTs (47 μg mL^{-1}) in a mixture of DMSO/H_2O (0.1:9). The inset shows the spectrum of a 0.5 mM solution of DPA in acetonitrile.

As mentioned earlier, DPA exhibits an intense blue fluorescence with a quantum yield approaching unity in many organic solvents.[39,40] In addition, sSWNTs quench the fluorescence of DPA. Figure 7 shows the decrease in the intensity of the DPA fluorescence in acetonitrile solution as the concentration of sSWNTs increases in the ng ml^{-1} range.

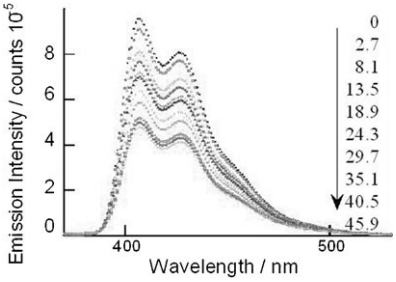

Figure 7. Fluorescence spectra (λ_{ex} = 370 nm) of a nitrogen-purged 70 μM solution of DPA in acetonitrile (1 × 1 cm^2 cuvette) upon addition of an increasing concentration of sSWNTs, as indicated (in ng mL^{-1}).

Precedents for the fluorescence quenching of anthracene by SWNTs due to interaction with the graphene walls can be found in the literature.[54,55]

As sSWNTs have a continuum absorption that includes the wavelength for DPA excitation ($\lambda_{ex}=370$ nm), it is inevitable that some of the decrease in the DPA fluorescence will be due to an internal filter effect caused by sSWNTs decreasing the number of photons absorbed by DPA. We notice, however, that low sSWNT concentrations were maintained in the experiments and, therefore, this effect is expected to be minor.

To provide convincing evidence for DPA fluorescence quenching by sSWNTs, the fluorescence lifetimes of DPA in acetonitrile and DPA in the presence of 15.3 ng mL^{-1} of sSWNTs were measured. Figure 8 shows the time profiles of

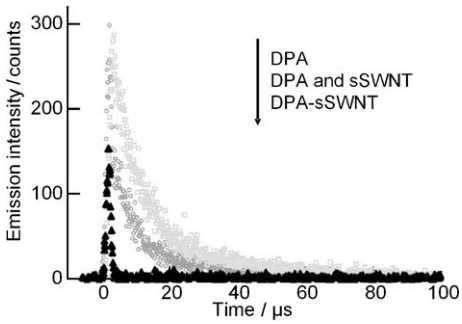

Figure 8. Time profiles of the emission ($\lambda_{ex}=370$ nm) at 420 nm of a 70 μM solution of DPA in acetonitrile in the absence and presence of sSWNTs (15.3 ng mL^{-1}) and that of a DMSO/D_2O (0.1:10) solution of DPA-sSWNTs (33.3 ng mL^{-1}).

the emissions. In the case of DPA in acetonitrile in the absence of sSWNTs, the emission–time profile fits well with a mono-exponential decay with a half-life of 7.5 ns, in good agreement with the τ value reported in the literature.[42] In comparison, when sSWNTs are present, the emission decays faster, following biexponential kinetics with lifetimes of 0.2 and 7.5 ns and relative contributions of 83 and 17%, respectively. It is tempting to interpret these kinetic data as reflecting the presence of two emitting DPA populations, that is, one (83%) in close proximity to the sSWNTs, being quenched by it, and another (17%) that emits without the influence of the sSWNTs. In this context it is worth noting that the diffusion coefficient of polymeric species (as sSWNTs) in organic solvents is low and that the DPA singlets are short-lived species. Overall, these kinetic measurements clearly demonstrate that sSWNTs interact with DPA in its singlet excited state and that the decrease in fluorescence intensity is mainly due to quenching rather an internal filter effect. With the data present in Figure 8, the steady-state fluorescence quenching gives a Stern–Volmer constant K_{SV} for the sSWNTs of 0.0179 mL ng^{-1}.

By using the emission of DPA in acetonitrile as a reference, we measured the fluorescence of an aqueous solution of DPA-sSWNTs at a concentration that matches the 370 nm absorbance of the DPA standard. Owing to the structure of DPA-sSWNTs and the low DPA content, it is estimated that in an optically matched solution, about 15% of the absorbance is due to DPA and 85% is due to the sSWNT backbone. It was observed that although the emission corresponds to the fluorescence of the DPA units present in DPA-sSWNTs lacking fine structure, the emission of DPA-sSWNTs is dramatically weaker with an overall quantum yield of 1.5×10^{-3} which, after correction for the fact that only 15% of the photons are absorbed by DPA, gives 1.0×10^{-2} (Figure 9). On the basis of the fluorescence

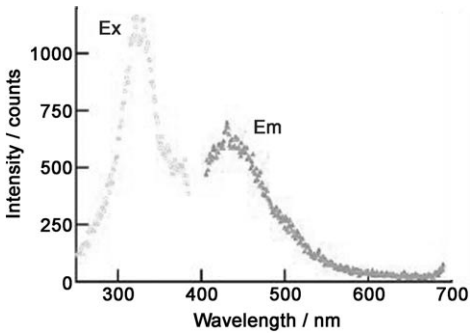

Figure 9. Emission (Em, $\lambda_{ex}=370$ nm) and excitation (Ex, $\lambda_{em}=430$ nm) spectra of a solution of DPA-sSWNTs (33.3 ng ml^{-1}) in DMSO/D_2O (0.1:10).

quenching experiments shown in Figure 7, the reduction in the emission of DPA caused by sSWNTs covalently bonded to DPA is more than expected based on the measurements of independent DPA and sSWNTs.

Assuming that the Stern–Volmer equation obtained for independent DPA and sSWNTs would apply to DPA-sSWNTs, the emission would be equivalent to that of DPA in the presence of 100 ng mL^{-1} sSWNTs, that is, about three times the total concentration of sSWNTs in the sample.

Furthermore, the time profile of the DPA-sSWNT emission is even shorter-lived than that recorded for DPA in the presence of 15.3 ng mL^{-1} sSWNTs. Thus, the lifetime for the DPA-sSWNT emission is below the response limit of our single-photon counting equipment, that is, $\tau<0.2$ ns (see Figure 8). Comparison of the emission parameters of DPA-sSWNTs with those measured for the sSWNT quenching of DPA allows the conclusion to be drawn that although the effect of the presence of sSWNTs follows the same trend whether or not the attachment is covalent or non-covalent, the covalent linkage significantly increases the efficiency of the interaction of sSWNTs with DPA. Thus, covalent binding of DPA to sSWNTs strongly reinforces an interaction that also occurs in the absence of the covalent linkage.

Laser flash photolysis of DPA and quenching of DPA triplets by sSWNTs: Laser excitation at 355 nm of a nitrogen-purged solution of DPA in DMSO gives rise to the generation of a transient decaying in the microsecond timescale which can be attributed to DPA triplets, in agreement with

the literature[42] (Figure 10). The signal decay follows first-order kinetics with a half-life of 1.1 μs and is quenched by oxygen (inset of Figure 10).

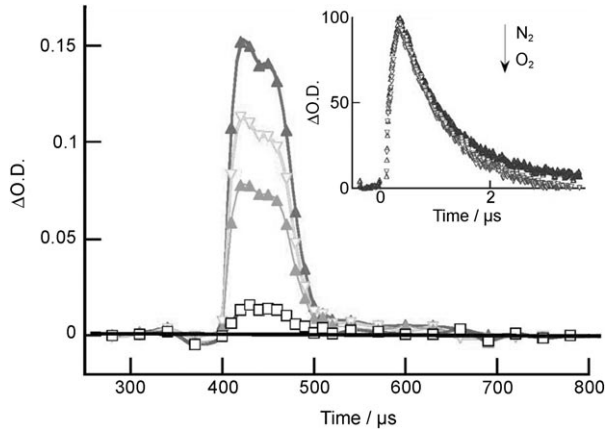

Figure 10. Transient spectra recorded for a nitrogen-purged 0.11 mM solution of DPA in DMSO/D_2O (1:1.5) measured 0.4, 0.8, 1.1 and 2.5 μs (traces from top to bottom) after 355 nm laser excitation. The inset shows the signal decay monitored at 420 nm after nitrogen- or oxygen-purging of the solution.

The DPA triplet excited state is quenched by sSWNTs (Figure 11), although the generation of some other transient, particularly the corresponding $DPA^{\cdot+}$ radical cation, was not observed. Thus, in contrast to the vast majority of the reports on the photochemistry of SWNTs, in which photoinduced electron transfer and the generation of long-lived charge-separated states occur, in the case considered here the quenching mechanism must operate by energy transfer from the DPA triplets to the sSWNTs. In addition, the quenching of the DPA triplet appears to occur through a static mechanism as it is the initial intensity of the signal after the laser flash and not the decay kinetics of the signal that changes upon addition of increasing amounts of sSWNTs.

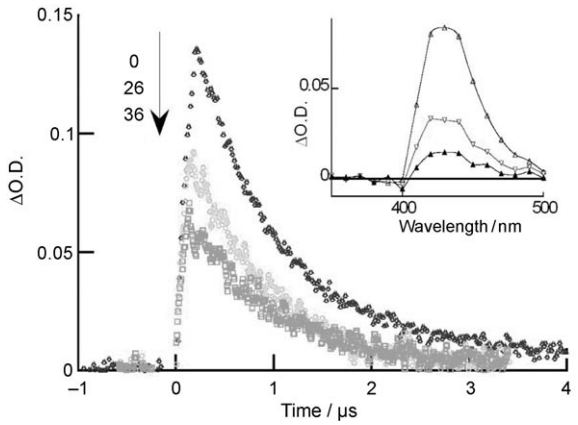

Figure 11. Quenching of DPA triplets by sSWNTs (concentrations given in ng mL^{-1}) monitored at 420 nm. The triplet was generated by 355 nm laser excitation (7 ns fwhp, 5 mJ per pulse) of a nitrogen-purged DPA solution (0.11 mM) in DMSO/D_2O (1:1.5). The inset shows the transient spectra recorded for the DPA solution in the presence of 36 ng mL^{-1} of sSWNTs 0.5, 1.2 and 2.0 μs (traces from top to bottom) after the laser pulse.

In contrast to the transient observed upon photolysis of DPA in the absence or presence of sSWNTs, laser flash photolysis of DPA-sSWNTs in D_2O shows a transient absorption across the entire wavelength range of 300–800 nm (Figure 12).

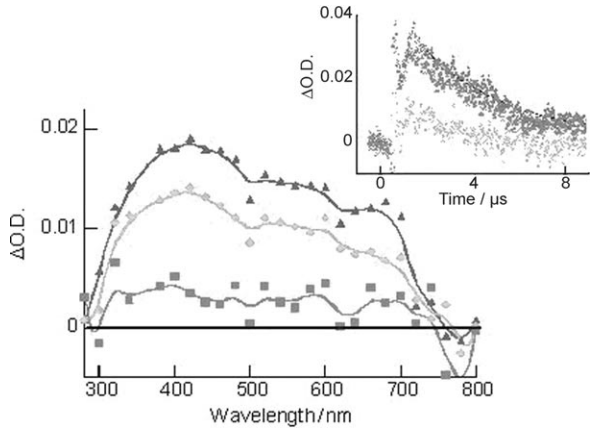

Figure 12. Time-resolved optical spectra recorded 1.2, 2.2 and 5.5 μs (traces from top to bottom) after 355 nm laser excitation of a nitrogen-purged 47 μg mL^{-1} solution of DPA-sSWNTs in DMSO/D_2O (3:10). The inset shows (from top to bottom) the time profile of the signal monitored at 400, 500 and 600 nm.

The signals shown in Figure 12 reveal overlapping components. Of these, the DPA triplet state contributes significantly to the signals at 400–500 nm, with an approximate lifetime of 2.8 μs, a reasonable value for the triplet state under these conditions. Beyond this, there are clearly other absorptions with lifetimes in the microsecond range. In particular, signals in the 650–750 nm region are probably dominated by the radical cation of DPA.[56] We anticipate that the electron will bind to the sSWNT, yielding a featureless absorption at 400–1400 nm, that is, across the entire spectral range.[57–59] In summary, the complex behaviour shown in Figure 12 is consistent with the triplet state of DPA and the electron-hole pair that results from excited-state electron transfer. In this way, the time-resolved spectrum of DPA-sSWNTs upon 355 nm excitation shows clear evidence for a specific interaction between DPA and the sSWNTs that is not observed upon photolysis of solutions containing both components (see inset in Figure 11). This confirms that the covalent bond reinforces the interaction between the two units.

Recent reports have revealed that reduced SWNTs exhibit a broad absorption across the entire UV/Vis region without having a characteristic peak that could serve to safely identify the species.[58,60,61] It has been found that variation of the van Hove bands in the NIR region can be used to firmly identify electrons localised on SWNTs.[58,60–62] However, we note that the NIR region is outside the range of con-

ventional photomultiplier tubes of time-resolved set-ups, which limits the utility of the time variations of the van Hove bands. In addition, as we have already mentioned when discussing the optical spectra of sSWNTs, they do not exhibit NIR bands that can be attributed to the van Hove singularities.

To find alternative evidence for the occurrence of photoinduced electron transfer upon excitation of DPA-sSWNTs, we performed a quenching study of the electron localised on a sSWNT by using methyl viologen (MV^{2+}). MV^{2+} is a good electron-acceptor[63] and it is anticipated that electrons will migrate from SWNTs to MV^{2+} to generate the corresponding radical cation. $MV^{\bullet+}$ is a long-lived species that is easily characterised by optical spectroscopy; its absorption spectrum consists of a sharp peak at 390 nm with a shoulder on the shorter wavelength side that is accompanied by a broad, less intense and structured band in the range 500–700 nm.[63] As anticipated, laser flash photolysis of DPA-sSWNTs in the presence of MV^{2+} gives rise to a transient spectrum (Figure 13) that consists of bands compatible with the presence of $MV^{\bullet+}$. A blank control at 355 nm reveals that no $MV^{\bullet+}$ is formed in the absence of DPA-sSWNTs.

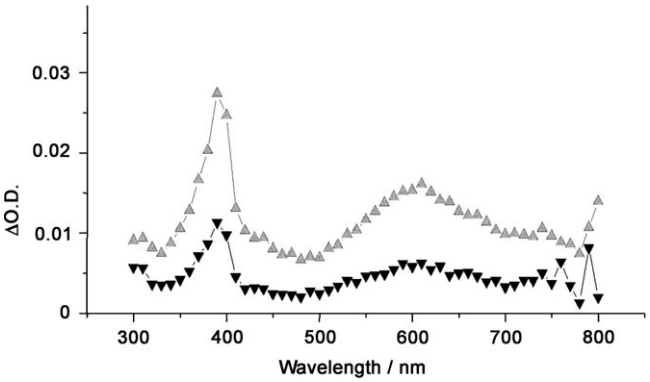

Figure 13. Transient spectra recorded 5.3 (top) and 167 μs (bottom) after 355 nm laser excitation of a nitrogen-purged 47 μg mL^{-1} solution of DPA-sSWNTs in DMSO/D_2O (3:10) upon addition of 100 μL of MV^{2+} (0.46 mg mL^{-1}). The inset shows the signal decay monitored at 600 nm.

Near-IR emission of DPA-sSWNTs: sSWNTs (λ_{ex} from 370 to 460 nm) barely emit in the visible region, but exhibit a very important emission in the near-IR (NIR).[58,64,65] As could have been anticipated based on the behaviour of sSWNTs, DMSO/D_2O solutions of DPA-sSWNTs exhibit NIR emission upon excitation at 266 nm. Figure 14 shows the emission spectra recorded for a solution of DPA-sSWNTs in DMSO/D_2O. Like the spectrum recorded for sSWNTs, the NIR emission of DPA-sSWNTs shows a structured emission across the entire NIR spectral range available to our system.

The intensity and time profile of the emission is not affected by the presence of oxygen. By exciting optically matched solutions of DPA-sSWNTs and sSWNTs at 266 nm it was observed that the NIR emission intensity of DPA-sSWNTs is a factor of 1.46 higher than that of sSWNTs.

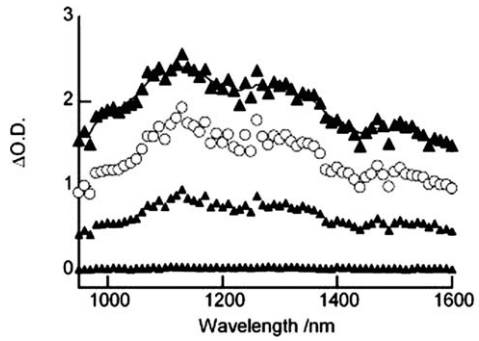

Figure 14. NIR emission recorded 3.5, 6.2, 10.5 and 50.0 μs (traces from top to bottom) after 266 nm laser excitation of a nitrogen-purged 47 μg mL^{-1} solution of DPA-sSWNTs in DMSO/D_2O (0.1:10).

Considering that the quantum yield of the sSWNT NIR emission has been estimated by us to be $(3.9\pm0.5)\times10^{-3}$,[66] based on the NIR emission of singlet oxygen as a reference, the quantum yield calculated for DPA-sSWNTs is $(5.7\pm0.5)\times10^{-3}$ in our detection window. Full spectrum quantum yields are anticipated to be higher. The higher NIR quantum yield of DPA-sSWNTs with respect to the precursor sSWNTs points to the photosensitisation by DPA of the nanotube walls. This energy transfer agrees with previous DPA excited state quenching commented upon earlier, the increased NIR emission quantum yield of sSWNTs being the result of this energy transfer.

The time profile of the emission in the region of 1100–1400 nm corresponds well with first-order kinetics and shows a half-life of 15.6 μs, which is very much similar to that of the sSWNT precursor (13.9 μs). These facts strongly suggest that the emission arises from a single species that is longer lived than the transients observed by absorption spectroscopy.

Conclusion

The functionalisation of short, soluble single-walled carbon nanotubes can serve to prepare responsive macromolecular entities that exhibit unique properties. The preparation of soluble species enables their analysis by routine liquid-phase ^{1}H NMR spectroscopy. The covalent linkage between DPA and sSWNT units is firmly supported by the shift in the NMR signals of DPA-sSWNTs relative to those of the DPA precursor. The steady-state and time-resolved fluorescence studies proved that quenching of DPA excited states by sSWNTs occurs even in the absence of covalent bonding, but is enhanced in DPA-sSWNTs. This interaction between DPA singlets and sSWNTs occurs predominantly by energy transfer, although the transient spectrum of DPA-sSWNTs exhibits features that suggest some photoinduced electron transfer occurs. Finally, we have observed NIR emission from DPA-sSWNTs that exhibits analogous features, albeit with a somewhat higher quantum yield, to that from sSWNTs.

Experimental Section

Preparation of DPA-sSWNTs: DPA and mercaptoethylamido-functionalised sSWNTs were synthesised as reported previously.[20,48] Anhydrous argon-purged toluene (5 mL) was added to a mixture of DPA (50 mg), AIBN (20 mg) and mercaptoethylamido-functionalised sSWNTs (100 mg) and the mixture was sonicated for 1 h to obtain a black dispersion. After stirring at reflux under an argon atmosphere for 48 h, the reaction mixture was diluted with toluene and filtered through a 0.2 μm PTFE membrane. The isolated black material was washed exhaustively several times with toluene, redispersed by sonication in toluene and finally centrifuged at 15000 rpm for 2 h. After this time, the solvent was decanted and the DPA-sSWNTs washed again with a mixture of toluene and diethyl ether (10:1). The samples were then dried at 30 °C for 1 day. The functionalised nanotubes were quite soluble in DMSO, giving a dark solution. The ^{1}H NMR spectrum of DPA-sSWNTs (Figure 2) was recorded in [D_6]DMSO with TMS as the internal standard. sSWNTs are readily soluble in D_2O. In the case of DPA-sSWNTs, a known weight was first dissolved in DMSO and the resulting solution diluted with D_2O to the required volume.

The resulting diphenylanthracene-functionalised nanotubes (DPA-sSWNTs) were characterised by ^{1}H NMR spectroscopy (Varian Gemini 300 MHz spectrometer) (Figure 2).

^{1}H NMR ([D_6]DMSO, 400 MHz): $\delta = 1.90$ (brt, 2H), 2.38 (t, 2H), 3.36 (brt, 2H), 3.44 (brt, 2H), 7.138 (d, $J = 7.2$ Hz, 2H, ArH), 7.176 (d, $J = 7.2$ Hz, 2H, ArH), 7.244 (d, $J = 7.2$ Hz, 2H, ArH), 7.262 ppm (d, $J = 7.2$, 2H, ArH).

Photophysical measurements: Steady-state fluorescence spectra were recorded in a PTI spectrofluorimeter in septum-capped Suprasil quartz cuvettes after purging the samples with nitrogen for at least 15 min before the experiments. Time-resolved fluorescence measurements were carried out by single-photon counting with an EasyLife PTI set-up and a 370 nm diode as the excitation source. Neutral density filters were used to attenuate the response to the required range. The time response of the equipment was determined using a cuvette containing glass wool as a scatterer. The system's software was also used to perform the curve-fitting.

Laser flash photolysis experiments were carried out with a LuzChem LFP-111 System and the third harmonic of a Nd/YAG laser (Minilite-II, 355 nm, 7 ns fwhp, 5 mJ per pulse) as the excitation source. The samples were diluted to an absorbance of around 0.3 units and then placed in 1×1 cm^2 cuvettes capped with septa which were purged with N_2 or O_2 for at least 15 min before the measurements were taken. NIR emission studies were carried out using a Peltier-cooled (−62 °C) Hamamatsu NIR detector operating at 900 V coupled with a computer-controlled grating monochromator. For excitation, the fourth harmonic (266 nm, 7 ns fwhh, 50 mJ per pulse) of the primary beam of a Nd/YAG laser or an Nd/YAG pumped OPO operating at 540 nm (7 ns fwhh, 40 mJ per pulse) was used. The solutions were placed in 1×1 cm^2 Suprasil quartz cuvettes capped with septa. The solutions were purged with N_2 or O_2 for at least 15 min before use. The system was controlled with a PC computer operating LuzChem LFPv3 software.

Acknowledgements

Financial support by the Spanish DGI (CTQ2006-06859) and the NSERC is gratefully acknowledged. C.A. and R.M. also thank the Spanish Ministry of Science and Education for a Juan de la Cierva research associate contract and a postgraduate scholarship, respectively. H.G. also acknowledges financial support (PR2007-0272) for his stay at the University of Ottawa. We thank Michel Grenier for technical assistance.

[1] F. Diederich, Y. Rubin, *Angew. Chem.* **1992**, *104*, 1123; *Angew. Chem. Int. Ed. Engl.* **1992**, *31*, 1101.
[2] E. H. L. Falcao, F. Wudl, *J. Chem. Technol. Biotechnol.* **2007**, *82*, 524.
[3] R. F. Curl, *Angew. Chem.* **1997**, *109*, 1636; *Angew. Chem. Int. Ed. Engl.* **1997**, *36*, 1567.
[4] M. Prato, *J. Mater. Chem.* **1997**, *7*, 1097.
[5] R. E. Smalley, *Angew. Chem.* **1997**, *109*, 1666; *Angew. Chem. Int. Ed. Engl.* **1997**, *36*, 1595.
[6] H. J. Dai, *Acc. Chem. Res.* **2002**, *35*, 1035.
[7] M. Anantram, L. Delzeit, A. Cassell, J. Han, M. Meyyappan, *Physica E (Amsterdam)* **2001**, *11*, 118.
[8] D. M. Guldi, A. Rahman, V. Sgobba, C. Ehli, *Chem. Soc. Rev.* **2006**, *35*, 471.
[9] D. M. Guldi, *Nature* **2007**, *447*, 50.
[10] G. Pagona, N. Tagmatarchis, *Curr. Med. Chem.* **2006**, *13*, 1789.
[11] D. Tasis, N. Tagmatarchis, A. Bianco, M. Prato, *Chem. Rev.* **2006**, *106*, 1105.
[12] J. Liu, A. G. Rinzler, H. J. Dai, J. H. Hafner, R. K. Bradley, P. J. Boul, A. Lu, T. Iverson, K. Shelimov, C. B. Huffman, F. Rodriguez-Macias, Y. S. Shon, T. R. Lee, D. T. Colbert, R. E. Smalley, *Science* **1998**, *280*, 1253.
[13] D. Tasis, N. Tagmatarchis, V. Georgakilas, M. Prato, *Chem. Eur. J.* **2003**, *9*, 4001.
[14] N. Nakashima, T. Fujigaya, *Chem. Lett.* **2007**, *36*, 692.
[15] H. Murakami, N. Nakashima, *J. Nanosci. Nanotechnol.* **2006**, *6*, 16.
[16] J. L. Hudson, M. J. Casavant, J. M. Tour, *J. Am. Chem. Soc.* **2004**, *126*, 11158.
[17] Y. P. Sun, K. F. Fu, Y. Lin, W. J. Huang, *Acc. Chem. Res.* **2002**, *35*, 1096.
[18] A. Hirsch, O. Vostrowsky, *Top. Curr. Chem.* **2005**, *245*, 193.
[19] A. Hirsch, *Angew. Chem.* **2002**, *114*, 1933; *Angew. Chem. Int. Ed.* **2002**, *41*, 1853.
[20] M. Alvaro, C. Aprile, B. Ferrer, H. Garcia, *J. Am. Chem. Soc.* **2007**, *129*, 5647.
[21] M. Alvaro, P. Atienzar, P. la Cruz, J. L. Delgado, V. Troiani, H. Garcia, F. Langa, A. Palkar, L. Echegoyen, *J. Am. Chem. Soc.* **2006**, *128*, 6626.
[22] S. Gotovac, Y. Hattori, D. Noguchi, J. Miyamoto, M. Kanamaru, S. Utsumi, H. Kanoh, K. Kaneko, *J. Phys. Chem. B* **2006**, *110*, 16219.
[23] M. A. Hamon, H. Hui, P. Bhowmik, H. M. E. Itkis, R. C. Haddon, *Appl. Phys. A* **2002**, *74*, 333.
[24] J. L. Bahr, J. M. Tour, *J. Mater. Chem.* **2002**, *12*, 1952.
[25] K. Balasubramanian, M. Burghard, *Small* **2005**, *1*, 180.
[26] R. Smajda, Z. Gyori, A. Sapi, M. Veres, A. Oszko, J. Kis-Csitari, A. Kukovecz, Z. Konya, I. Kiricsi, *J. Mol. Struct.* **2007**, *834*, 471.
[27] M. Lucci, R. Regoliosi, A. Reale, A. Di Carlo, S. Orlanducci, E. Tamburri, M. L. Terranova, P. Lugli, C. Di Natale, A. D′Amico, R. Paolesse, *Sens. Actuators, B* **2005**, *111*, 181.
[28] M. Lucci, A. Reale, A. Di Carlo, S. Orlanducci, E. Tamburri, M. L. Terranova, I. Davoli, C. Di Natale, A. D′Amico, R. Paolesse, *Sens. Actuators, B* **2006**, *118*, 226.
[29] H. N. Choi, J. Y. Lee, Y. K. Lyu, W. Y. Lee, *Anal. Chim. Acta* **2006**, *565*, 48.
[30] A. Merkoci, M. Pumera, X. Llopis, B. Perez, M. del Valle, S. Alegret, *TrAC Trends Anal. Chem.* **2005**, *25*, 826.
[31] E. Kymakis, G. A. J. Amaratunga, *Appl. Phys. Lett.* **2002**, *80*, 112.
[32] E. Kymakis, G. A. J. Amaratunga, *Sol. Energy Mater. Sol. Cell* **2003**, *80*, 465.
[33] E. Kymakis, I. Alexandrou, G. A. J. Amaratunga, *J. Appl. Phys.* **2003**, *93*, 1764.
[34] S. Bhattacharyya, E. Kymakis, G. A. J. Amaratunga, *Chem. Mater.* **2004**, *16*, 4819.
[35] P. Castrucci, F. Tombolini, M. Scarselli, E. Speiser, S. Del Gobbo, W. Richter, M. De Crescenzi, M. Diociaiuti, E. Gatto, M. Venanzi, *Appl. Phys. Lett.* **2006**, *89*.
[36] D. M. Guldi, G. M. A. Rahman, M. Prato, N. Jux, S. H. Qin, W. Ford, *Angew. Chem.* **2005**, *117*, 2051; *Angew. Chem. Int. Ed.* **2005**, *44*, 2015.
[37] S. Kazaoui, N. Minami, B. Nalini, Y. Kim, K. Hara, *J. Appl. Phys.* **2005**, *98*.

[38] R. L. Patyk, B. S. Lomba, A. F. Nogueira, C. A. Furtado, A. P. Santos, R. M. Q. Mello, L. Micaroni, I. A. Hummelgen, *Phys. Status Solidi RRL* **2007**, *1*, R43.
[39] J. V. Morris, M. A. Mahaney, J. R. Huber, *J. Phys. Chem.* **1976**, *80*, 969.
[40] L. F. V. Ferreira, S. M. B. Costa, E. J. Pereira, *J. Photochem. Photobiol. A* **1991**, *55*, 361.
[41] J. D. Debad, S. K. Lee, X. X. Qiao, R. A. Pascal, A. J. Bard, *Acta Chem. Scand.* **1998**, *52*, 45.
[42] T. Suzuki, M. Nagano, S. Watanabe, T. Ichimura, *J. Photochem. Photobiol. A* **2000**, *136*, 7.
[43] W. R. Ware, W. Rothman, *Chem. Phys. Lett.* **1976**, *39*, 449.
[44] Y. H. Kim, S. K. Kwon, *J. Appl. Polym. Sci.* **2006**, *100*, 2151.
[45] B. Balaganesan, W. J. Shen, C. H. Chen, *Tetrahedron Lett.* **2003**, *44*, 5747.
[46] Z. H. Xu, Y. Wu, B. Hu, I. N. Ivanov, D. B. Geohegan, *Appl. Phys. Lett.* **2005**, *87*.
[47] M. Monthioux, B. W. Smith, B. Burteaux, A. Claye, J. E. Fischer, D. E. Luzzi, *Carbon* **2001**, *39*, 1251.
[48] A. Corma, H. Garcia, *Adv. Synth. Catal.* **2006**, *348*, 1391.
[49] M. Alvaro, M. Benitez, J. F. Cabeza, H. Garcia, A. Leyva, *J. Phys. Chem. C* **2007**, *111*, 7532.
[50] M. Alvaro, P. Atienzar, P. de la Cruz, J. L. Delgado, H. Garcia, F. Langa, *Chem. Phys. Lett.* **2004**, *386*, 342.
[51] K. A. S. Fernando, Y. Lin, W. Wang, S. Kumar, B. Zhou, S.-Y. Xie, L. T. Cureton, Y.-P. Sun, *J. Am. Chem. Soc.* **2004**, *126*, 10234.
[52] A. G. Ryabenko, N. A. Kiselev, J. L. Hutchison, T. N. Moroz, S. S. Bukalov, L. A. Mikhalitsyn, R. O. Loutfy, A. P. Moravsky, *Carbon* **2007**, *45*, 1492.
[53] K. J. Lee, H. Lee, J. Y. Lee, S. C. Lim, K. H. An, Y. H. Lee, Y. S. Lee, *J. Korean Phys. Soc.* **2005**, *46*, 906.
[54] T. G. Hedderman, S. M. Keogh, G. Chambers, H. J. Byrne, *J. Phys. Chem. B* **2006**, *110*, 3895.
[55] M. J. Gomez-Escalonilla, P. Atienzar, J. L. Garcia Fierro, H. Garcia, F. Langa, *J. Mater. Chem.* **2008**, *18*, 1592.
[56] M. S. Workentin, L. J. Johnston, D. D. M. Wayner, V. D. Parker, *J. Am. Chem. Soc.* **1994**, *116*, 8279.
[57] D. M. Guldi, M. Marcaccio, D. Paolucci, F. Paolucci, N. Tagmatarchis, D. Tasis, E. Vazquez, M. Prato, *Angew. Chem.* **2003**, *115*, 4338; *Angew. Chem. Int. Ed.* **2003**, *42*, 4206.
[58] M. A. Herranz, N. Martin, S. P. Campidelli, M. Prato, G. Brehm, D. M. Guldi, *Angew. Chem.* **2006**, *118*, 4590; *Angew. Chem. Int. Ed.* **2006**, *45*, 4478.
[59] N. Tagmatarchis, M. Prato, D. M. Guldi, *Physica E (Amsterdam)* **2005**, *29*, 546.
[60] M. A. Herranz, C. Ehli, S. Campidelli, M. Gutierrez, G. L. Hug, K. Ohkubo, S. Fukuzumi, M. Prato, N. Martin, D. M. Guldi, *J. Am. Chem. Soc.* **2008**, *130*, 66.
[61] C. Ehli, S. Campidelli, F. G. Brunetti, M. Prato, D. M. Guldi, *J. Phorph. Phthal.* **2007**, *11*, 442.
[62] B. Ballesteros, G. de la Torre, C. Ehli, G. M. A. Rahman, F. Agullo-Rueda, D. M. Guldi, T. Torres, *J. Am. Chem. Soc.* **2007**, *129*, 5061.
[63] M. Alvaro, B. Ferrer, V. Fornes, H. Garcia, *Chem. Commun.* **2001**, 2546.
[64] F. Wang, G. Dukovic, L. E. Brus, T. F. Heinz, *Phys. Rev. Lett.* **2004**, *92*.
[65] L. Cognet, D. A. Tsyboulski, J.-D. R. Rocha, C. D. Doyle, J. M. Tour, R. B. Weisman, *Science* **2007**, *316*, 1465.
[66] C. Aprile, R. Martin, M. Alvaro, J. C. Scaiano, H. Garcia, *J. Phys. Chem, B* in press.

Received: January 30, 2008
Published online: April 16, 2008

